Journal of Thermal Analysis and Calorimetry, Vol. 87 (2007) 1, 165–169

SORPTION ON AS-SYNTHESIZED MCM-41

J. Goworek[1*], *A. Kierys*[1], *M. Iwan*[2] *and W. Stefaniak*[1]

[1]Maria Curie-Skłodowska University, Department of Adsorption, M. Curie-Skłodowska sq. 3, 20-031 Lublin, Poland
[2]Maria Curie-Skłodowska University, Department of General Chemistry, M. Curie-Skłodowska sq. 3, 20-031 Lublin, Poland

Mesoporous materials MCM-41 with the hexagonal arrangement of pores were obtained using dodecyltrimethylammonium bromide and octadecyltrimethylammonium bromide as templating surfactants. Adsorption of toluene and propan-1-ol on the as-synthesized MCM-41 silica samples was investigated using the TG-DTG, DTA and DSC techniques. The sorption mechanism of used adsorptives is discussed in terms of hydrophobicity of pore interior filled with template as well as pore dimensions.

Keywords: *adsorption, DSC, DTA, MCM-41, TG-DTG*

Introduction

MCM-41 silica exhibits hexagonal arrays of uniform and cylindrical mesopores with diameters in the range 1.5–10 nm. The pore dimensions may be controlled by a choice of appropriate synthesis conditions [1–8]. Application of these materials is determined by sorption properties and pore dimensions. Similar to the case of amorphous silica gel on the MCM-41 surface isolated and hydrogen bounded silanol groups are present. The siloxane bridges formed in the last stage of synthesis procedure are assumed to be surface species of hydrophobic character. Thus, MCM-41 silica can sorb specifically polar molecules as well as aliphatic and aromatic hydrocarbons. Synthesis of MCM-41 is based on addition of an inorganic silica source (sodium silicate, tetraethoxysilane, fumed silica) to the solution containing the surfactant micellar template. In the final material the surfactant micelles are encapsulated in the silica skeleton. The internal pores become hollow after the organic phase has been removed. High temperature treatment in air causes degradation and evaporation of surfactant molecules from the sample [9–11]. Evacuation of organic species is a complex process of exothermic character [12–15]. At the beginning of surfactant template removal below 473 K usually a small endothermic effect is observed which is ascribed to elimination of the trimethylamine group. However, the initial fragment of TG curve (T<373 K) represents desorption of water, which is confined probably in the silica skeleton.

The temperature ranges corresponding to the successive stages of template removal are not precisely specified due to their dependence on a heating rate. For higher heating rates the inflection points ascribed to appropriate phase transformations are shifted toward higher temperatures. Thermal treatment causes complete degradation of surfactant molecules and evaporation/combustion of various chemical species. Above 573 K oxidation of organic species and conversion to water and carbon dioxide take place. These processes are of exothermic character. Finally, we obtain MCM-41 silica without organics within pores. The pure siliceous MCM-41 exhibits strong adsorption properties in relation to many adsorptives [16–20]. However, some experiments demonstrate sorption of various substances by as-synthesized samples whose pores are filled with organic template [21, 22]. In [21] significant adsorption of benzene is reported for MCM-41 synthesized using surfactants of various length of hydrocarbon chain. The amount adsorbed was practically independent of a number of carbon atoms in the surfactant molecule. In the present paper we focused on adsorption of toluene and propan-1-ol on MCM-41 synthesized using dodecyl and octadecyltrimethylammonium bromide. The saturated samples of these materials with both adsorptives were studied using thermogravimetry (TG-DTG), differential thermal analysis (DTA) and differential scanning calorimetry (DSC).

Experimental

Sample preparation

MCM-41(C_{12}) and MCM-41(C_{18}) materials were synthesized using dodecyl trimethylammonium bromide and octadecyltrimethylammonium bromide as surfactants (C_{12}TMAB, 99% Sigma; C_{18}TMAB, 98% Aldrich), respectively. The preparation procedure followed the method described in [23].

* Author for correspondence: jgoworek@hermes.umcs.lublin.pl

1388–6150/$20.00

Akadémiai Kiadó, Budapest, Hungary
Springer, Dordrecht, The Netherlands

Tetraethoxysilane (TEOS, 98% Fluka) was used as a silica source. The initial sample was dried at 373 K and used without further thermal treatment, thus the micellar filling was entirely preserved. The as-synthesized samples were exposed at 298 K to the vapor of toluene and propan-1-ol in a desiccator for 36 h. Before sorption experiment the air was evacuated from desiccator. Thus, one can assume that at equilibrium practically saturated (p/p_0≈0.99) vapors of adsorptive is present over the sample.

Methods

The mass loss curves and differential scanning calorimetry curves were measured using the Setaram Setsys 16/18 instrument, using the standard platinum crucible and the sample mass of ~10 mg. The samples were heated at a rate of 5 K min^{-1} from room temperature to 873 K in air flow of 0.6 dm^3 h^{-1}.

Nitrogen adsorption measurements were carried out using a volumetric adsorption analyzer ASAP 2405 (Micrometrics, Norcros, GA). The specific surface areas S_{BET}, were calculated using the BET method for the adsorption data in a relative pressure range p/p_0 from 0.05 to 0.25. Pore size and pore size distribution were determined using the BJH procedure [24].

Results and discussion

Porosity of siliceous skeleton for the studied MCM-41 samples was characterized from nitrogen adsorption data. Both samples were calcined at 823 K for 8 h and next kept at the same temperature for 5 h in oxygen stream. Low temperature adsorption/desorption isotherms for MCM-41(C_{12}) and MCM-41(C_{18}) are shown in Fig. 1.

For the both investigated samples the adsorption/desorption isotherms exhibit a typical shape (IV type of isotherm) for uniform porosity with a well-resolved step at relative pressure p/p_0≈0.2 and 0.4, respectively. This step corresponds to condensation in the primary-hexagonally arranged pores. In Fig. 1 the nitrogen adsorption/desorption isotherm for the as-synthesized MCM-41(C_{18}) material is also shown. As it is seen, the adsorption in this case is negligibly small and represents only external interparticle surface. The small hysteresis loop (larger for the MCM-41(C_{18}) sample) is observed above p/p_0=0.85. The external specific surface area consists of 2–3% of the total specific surface area of the samples investigated after calcination. The structural parameters derived from the adsorption/desorption data are collected in Table 1.

The specific surface area S_{BET} was calculated using the BET method for adsorption data in a relative pressure range from 0.05 to 0.25. The pore volume of primary pores V_p^* for the samples under study was derived from adsorption at a relative pressure of 0.45 i.e. at the end of condensation in these pores. The total pore volume V_p was derived from the single point adsorption at p/p_0=0.98. The pore size distribution PSD was calculated using the BJH method. The presented results of adsorption experiments confirm the dependence of pore diameter on the length of hydrocarbon chain in the surfactant molecule. The increase of the number of carbon atoms from C_{12} to C_{18} causes the increase of the mean pore diameter from 20.0 to 28.7 nm. Thus, the pore interior of as-synthesized MCM-41(C_{18}) contains larger amount of hydrophobic species as compared to the MCM-41(C_{12}) sample. The small adsorption of nitrogen on as-synthesized MCM-41 testifies that the nitrogen is adsorbed only on the external surface of particles and does not penetrate into pores filled with organic template.

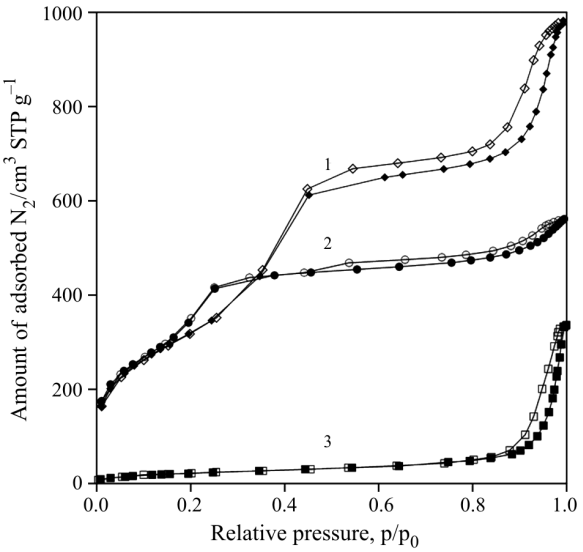

Fig. 1 Nitrogen adsorption/desorption isotherms at 77 K for the silica samples under study; 1 – MCM-41(C_{18}) calcined, 2 – MCM-41(C_{12}) calcined, 3 – as-synthesized MCM-41(C_{18})

Sorption capacity of the hydrophobic surfactant core of as-synthesized samples under study was investigated using toluene and propan-1-ol as adsorptives. The thermodesorption TG curves as well as the DSC curves for as-synthesized MCM-41(C_{18}) and saturated with toluene MCM-41(C_{12}) and MCM-41(C_{18}) are shown in

Table 1 Structural parameters obtained from the nitrogen adsorption data for investigated MCM-41 samples

Sample	S_{BET}/ m^2 g^{-1}	D_{BJH}/ Å	V_p/ cm^3 g^{-1}	V_p^*/ cm^3 g^{-1}
MCM-41(C_{12})	1214	20.0	0.85	0.39
MCM-41(C_{18})	1146	28.7	1.48	0.68

*the volume of primary pores

Figs 2–4. However, the TG curves and the DTA curves corresponding to them for as-synthesized MCM-41(C_{12}) and saturated with propan-1-ol MCM-41(C_{12}) and MCM-41(C_{18}) are presented in Figs 5–7. It follows from the TG curves presented in Figs 2 and 5 that the mass of template consists of 52 and 37% of the total mass of the MCM-41(C_{18}) and MCM-41(C_{12}) samples, respectively. Thus, relative contamination of siliceous material is higher in the case of MCM-41(C_{12}). Consequently, mass loss representing desorption of water at the beginning of thermal treatment is higher for this material (Fig. 5). Exothermic combustion above 573 K corresponding to step III on the TG curves is much higher for MCM-41(C_{18}) in comparison to MCM-41(C_{12}) (Figs 3 and 4). It means that after the same time period the MCM-41(C_{12}) sample contains relatively smaller amount of organic species deposited in the pore interior. Moreover, mass losses represented by step II are for both materials almost identical. It suggests much faster template removal for the MCM-41(C_{12}) sample at the same heating rate.

For the initial MCM-41(C_{18}) sample one can observe in the first stage of thermal treatment in the temperature range from 298 to 383 K well resolved

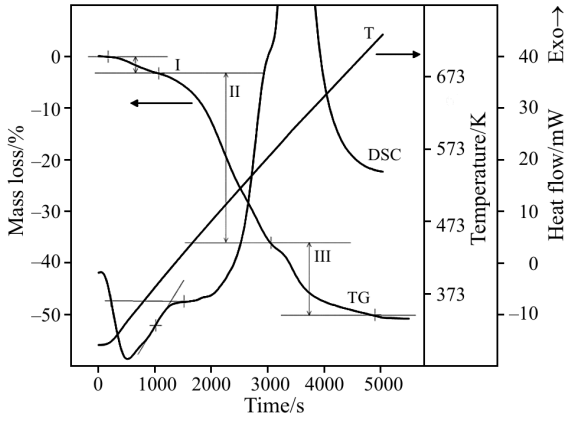

Fig. 2 TG and DSC curves for MCM-41(C_{18}) sample

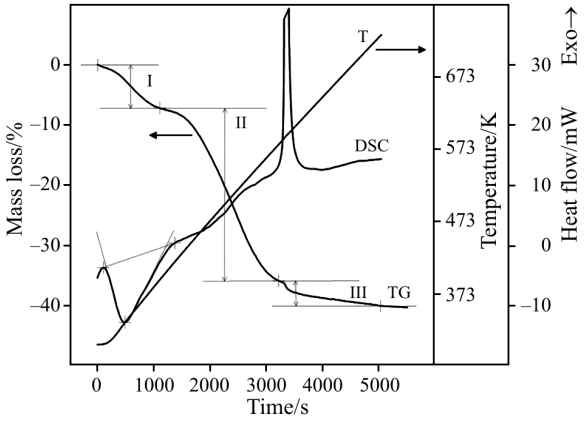

Fig. 3 TG and DSC curves for MCM-41(C_{12})–toluene

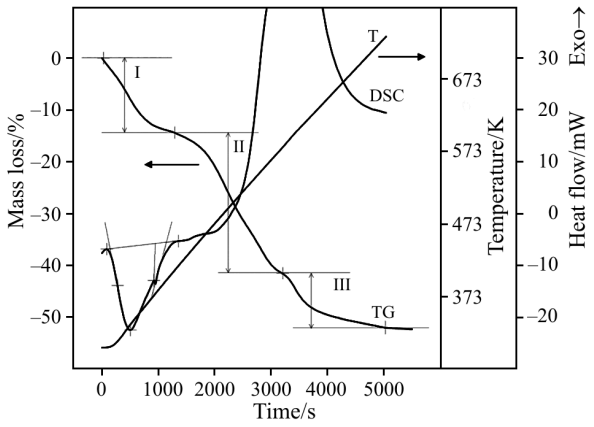

Fig. 4 TG and DSC curves for MCM-41(C_{18})–toluene

endothermic peak representing desorption of water. About 3% *w*/*w* mass loss is detected. However, for the samples saturated with toluene, the mass loss steps in the same temperature range are ~7.5 and ~14.5% for MCM-41(C_{12}) and MCM-41(C_{18}), respectively. Two next mass loss steps for all samples represent decomposition of surfactant. They are accompanied by exothermic effects and were widely discussed elsewhere [12–16].

The desorption of water from MCM-41 exhibits a wide peak on the DSC curves. The similar peaks are present on the DSC curves for the MCM-41(C_{12}) and MCM-41(C_{18}) samples with adsorbed toluene. It is worth mentioning that endothermic effects are larger in the case of MCM-41(C_{12}) when the amount of adsorbed toluene is three times lower in comparison to the MCM-41(C_{18}) sample. Moreover, the DSC desorption peak for MCM-41(C_{18}) exhibits a bimodal character indicating that two independent processes overlap in the mentioned temperature range. It may suggest that toluene is involved in strong capillary as well as adsorption interactions with the silica framework. It is well known that when pore dimensions become smaller higher temperature of pore emptying is required. Taking into account the fact that the endothermic effect for the satu-

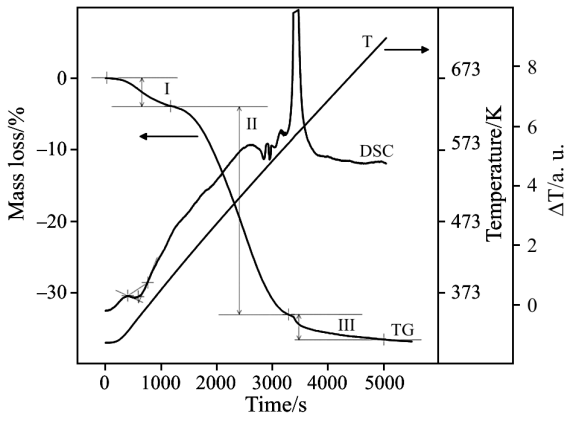

Fig. 5 TG and DTA curves for MCM-41(C_{12})

Table 2 Desorption of toluene and *n*-propanol from samples investigated

Sample	Desorbed amount/*w*/*w*%	
	toluene	propan-1-ol
MCM-41(C_{12})	3	4.8
MCM-41(C_{18})	11.5	27.7

rated sample is a sum of desorption energy of water and toluene and propan-1-ol one can assume that energy of desorption for these adsorptives is equal to the difference of both effects i.e. ΔH_{des}^{tol}=101.7 kJ g^{-1}, H_{des}^{prop}= 84.2 kJ g^{-1} for MCM-41(C_{12}) and ΔH_{des}^{tol}=19.7 kJ g^{-1}, H_{des}^{prop}=10.9 kJ g^{-1} for MCM-41(C_{18}).

The adsorption of propan-1-ol on MCM-41(C_{12}) and MCM-41(C_{18}) is much higher than that of toluene and is more differentiated for both samples (Table 2). Simultaneously, desorption of water and alcohol is pronounced on the DTA curves. On the DTA curves presented in Figs 5 and 6 below 373 K there is observed one peak for as-synthesized MCM-41(C_{12}) and bimodal one for as-synthesized MCM-41(C_{12}) saturated with alcohol. Thus, one can assume that the first peak at lower temperature represents desorption of propan-1-ol and the second one at higher temperature represents desorption of water. The volume of adsorbed propan-1-ol on MCM-41(C_{18}) corrected with respect to water contamination and calculated by converting of mass loss to the volume of the liquid adsorbate represents almost 30% of total volume of emptied pores (Fig. 7). It may suggest considerable swelling of hydrocarbon core of template being in contact with propan-1-ol vapour. On the other hand, enthalpy of desorption from smaller pores is higher than for desorption from larger ones. Thus, it may be assumed that the adsorption on as-synthesized MCM-41 is determined by adsorbate-micellar core interactions as well as pore dimensions.

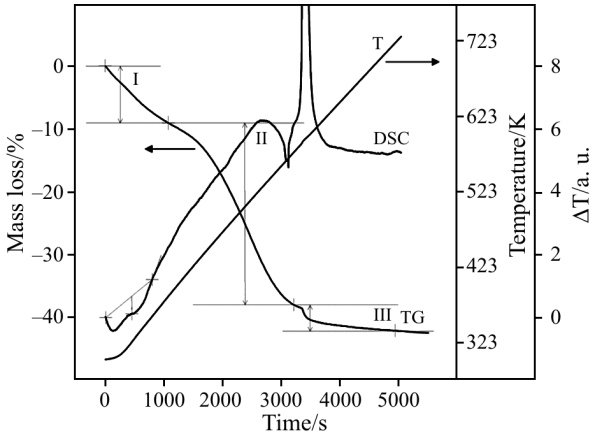

Fig. 6 TG and DTA curves for MCM-41(C_{12})–propan-1-ol

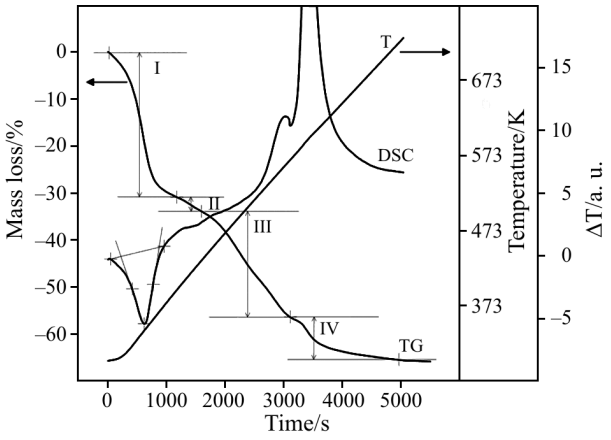

Fig. 7 TG and DTA curves for MCM-41(C_{18})–propan-1-ol

A big difference of propan-1-ol uptake for MCM-41(C_{12}) and MCM-41(C_{18}) is hard to explain. Probably, it is a result of different morphology of these materials. As follows from the nitrogen adsorption data MCM-41(C_{18}) is characterized by a large total pore volume (nitrogen adsorption/desorption isotherms shown in Fig. 1). A great part of this volume may be ascribed to wide mesopores corresponding to the interparticle voids (p/p_0>0.9). Thus, in part adsorption of propan-1-ol takes place on the external surface of silica particles which does not contain surfactant molecules and exhibit the presence of surface silanols. These silanols interact specifically with alcohol molecules. Thus, the adsorption of propan-1-ol in the micellar template is overestimated in this case.

Conclusions

The presented results show that the as-synthesized samples of MCM-41 containing micellar template inside pores exhibit specific sorption properties when exposed to vapour of various substances. The extent of adsorption on the non-calcined samples is much lower compared to adsorption on the calcined sample when the silica surface is totally accessible for adsorptives.

As the internal surface of the as-synthesized MCM-41 sample is not accessible for nitrogen molecules and simultaneously sorption of toluene and propan-1-ol takes place, one can conclude that uptake of these adsorptives is caused by their solubility in the micellar template. Adsorption is higher when dimensions of template core increases. Simultaneously, the desorption of toluene and propan-1-ol requires a higher energy for lower micellar core. In such a case the share of capillary interactions becomes larger in the sorption process.

References

1 C. T. Kresge, M. E. Leonowicz, W. J. Roth, J. C. Vartuli and J. S. Beck, Nature, 359 (1992) 710.
2 J. S. Beck, J. C. Vartuli, W. J. Roth, M. E. Leonowicz, C. T. Kresge, K. D. Schmitt, C. T.-W. Chu, D. H. Olson, E. W. Sheppard, S. B. McCullen, J. B. Higgins and J. L. Schlenker, J. Am. Chem. Soc., 114 (1992) 10834.
3 M. Sayari, P. Liu, M. Kruk and M. Jaroniec, Chem. Mater., 9 (1997) 2499.
4 N. Ulagappan and C. N. R. Rao, Chem. Commun., (1996) 2759.
5 Ch.-F. Cheng, W. Zhou and J. Klinowski, Chem. Phys. Lett., 263 (1996) 247.
6 M. Kruk, M. Jaroniec and M. Sayari, Langmuir, 13 (1997) 6267.
7 M. Kruk, M. Jaroniec and M. Sayari, J. Phys. Chem., 101 (1997) 583.
8 L. Chen, T. Horiouchi, T. Mori and K. Maeda, J. Phys. Chem., 103 (1999) 1216.
9 R. Denoyel, M. T. J. Keene, P. L. Llewellyn and J. Rouquerol, J. Therm. Anal. Cal., 56 (1999) 261.
10 S. A. Araujo, M. Ionashiro, V. J. Fernandes and A. S. Araujo, J. Therm. Anal. Cal., 64 (2001) 801.
11 M. J. B. Souza, A. O. S. Silva, J. M. F. B. Aquino, V. J. Fernandes and A. S. Araujo, J. Therm. Anal. Cal., 79 (2005) 493.
12 F. Kleitz, W. Schmidt and F. Schüth, Micropor. Mesopor. Mater., 44–45 (2001) 95.
13 F. Kleitz, W. Schmidt and F. Schüth, Micropor. Mesopor. Mater., 65 (2003) 1.
14 J. Goworek, A. Borówka, R. Zaleski and R. Kusak, J. Therm. Anal. Cal., 79 (2005) 555.
15 J. Ryczkowski, J. Goworek, W. Gac, S. Pasieczna and T. Borowiecki, Thermochim. Acta, 434 (2005) 2.
16 P. J. Branton, P. G. Hall and K. S. W. Sing, Adsorption, 1 (1995) 77.
17 X. S. Zhao, Q. Ma and G. Q. Lu, Energy Fuels, 12 (1998) 1051.
18 C. Nguyen, C. G. Sonwane, S. K. Bhatia and D. D. Do, Langmuir, 14 (1998) 4950.
19 J.-H. Yun, T. Düren, F. J. Keil and N. A. Seaton, Langmuir, 18 (2002) 2693.
20 P. J. Branton, P. A. Reynolds, A. Studer, K. S. W. Sing and J. W. White, Adsorption, 5 (1995) 91.
21 J. C. Vartuli, A. Malek, W. J. Roth, C. T. Kresge and S. B. McCullen, Micropor. Mesopor. Mater., 691 (2001) 44.
22 L. Mercier and T. J. Pinnavaia, Chem. Mater., 12 (2000) 188.
23 M. Grün, K. K. Unger, A. Matsumoto and K. Tsutsumi, Characterization of Porous Solids IV, B. McEnaney, J. T. Mays, J. Rouquerol, F. Rodriguez-Reinoso, K. S. W. Sing and K. K. Unger, Eds, The Royal Society of Chemistry, London 1997, p. 81.
24 E. P. Barrett, L. G. Joyner and P. P. Halenda, J. Am. Chem. Soc., 73 (1951) 373.

DOI: 10.1007/s10973-006-7810-0